DESIGN AND IMPLEMENTATION OF ARM CORTEX-M4 PROCESSOR BASED CLOSED LOOP CONTROL OF THREE PHASE INDUCTION MOTOR

[1]RAJAN.V.R
Assistant Professor, V V College of Engineering, Arasoor, Tisaiyanvilai, Thoothukudi, Tamil Nadu 628656, India, rajan.vrrp@gmail.com

[2]Dr. K. SELVI
Associate Professor, Thiagarajar College of Engineering, Madurai, Tamil Nadu, 625015, India
kseee@tce.edu

Abstract: *This article presents the design and implementation of open-loop and closed-loop control of a three phase induction motor using an ARM Cortex-M4 processor. This implementation includes proportional-integral (PI) control logic and sinusoidal pulse width modulation (SPWM) technique. The high processing speed of the ARM Cortex processor family permits the use of highly developed control to construct a high-precision control system. The design of the controller structure is achieved using a committed digital-based voltage/frequency (V/Hz) control scheme processor, specifically created for a motor that transform three-phase motor speed into control. This structure is composed of faster voltage/frequency control and generation of SPWM, which helps out to trigger the three-phase two-level inverter effectively. The calculation of frequency and voltage generated in the voltage source inverter will show its reliability and efficiency. The experimental authentication is carried out by open-loop and closed-loop volts per hertz control (V/f) technique. A graphical user interface screen is designed in MATLAB to set a reference speed as an input to the processor and monitor the real time performances through Ethernet connectivity. The electrical energy is used economically by adopting this implementation technique.*

Key words: Induction motor (IM), intelligent power module (IPM), sinusoidal pulse width modulation (SPWM), voltage/frequency control (V/f).

1. Introduction

The scope of the development of power electronic devices has been very quickly expanding. As majority of the applications in industry are automatic and dynamic, the efficiency and performance of the drive chiefly rely on the capacity of the controller unit of the system [1, 2]. Almost all the manufactory applications are run by an AC machine that is replaced by a DC one. So, it becomes essential to undertake a thorough investigation for a variable speed, variable frequency drive control methodology for the AC machine drive like an induction motor (IM) [3].

Many studies have been conducted on vector control because of its enhanced dynamic response [4-6]. Although scalar control [7, 8, 9] has a simple design, it exhibits a slow, steady-state error. Owing to the wide range of applications in the industry, scalar control system (V/f) is deliberated in this study. Generally, proportional–integral (PI) control method is employed in V/f control design for IMs. Many forms of inverter topology categorized with numerous phases, power of the switching device, commutation, switching scheme (PWM), and the output waveform generated are used to the variable-speed drive system design [10].

A number of digital and transistor logic circuits like microprocessor or microcontroller or digital signal processors (DSPs) can be used to evolve pulse width modulation (PWM) [11-13]. In [14], an embedded DSP-based (V/f) control using fuzzy system was developed. Tzou [15] presented robust control of an AC induction servo drive using a DSP. The control mechanism employed was based on internal model control (IMC) theory. Saad and Arrofiq [16] presented a modified-fuzzy-based scalar controller for PWM drive IM using programmable logic controller (PLC). In [17], Fuzzy PI controller-based (V/f) speed control of IM with a space vector pulse width modulation (SVPWM) using field programmable gate array (FPGA) was realized. The peak overshoot and the settling time were somewhat high. Hariram and Marimuthu [18] presented a digitized hardware design scheme of an SVPWM-based (V/f) control of IM using FPGA. In [19], the vector control of matrix converter based sensorless synchronous

reluctance motor has been implemented. In [20], design and implementation of an 8-bit microcontroller-based space vector PWM Inverter Fed (V/f) IM drive was realized. However microprocessor-based implementations have the demerits of complex circuitry, limited functions, sequential execution, and problem in circuit modification. Generally, the sequential execution curtails its speed. The shortcomings of digital PWM control [21] include simple circuitry, software control, and flexibility in adaptation to different applications. However, producing PWM gating signals and current control loops requires a high sampling rate in order to attain a wide-band width discharge [22]. Because advanced RISC machine(ARM) devices are 3-4 time more power efficient than x86 systems when considering the requests per second per watt relation under various load conditions [23], they are used in manufactory applications.

Recently, due to ARM Cortex-based PWM controllers it is feasible to combine complex analog and digital circuits easily and effectively. In [24], an ARM Cortex-M4-based robot control was implemented with a DC motor. In [25], development of embedded navigation and control system for unmanned aerial vehicle was realized. It was used in microcontrollers of ARM Cortex-M4 and written in C language. In [26], closed-loop control of DC motor using ARM Cortex-M3 processor by a proportional-integral-derivative (PID) controller was developed.

This article describes the design, development, and comparison of an open-loop and closed-loop control system of IM which is implemented on ARM Cortex-M4 processor. Because of the ARM Cortex-M4-based PWM controllers, it now feasible to integrate complicated analog and digital circuits by using a customized block set named "Waijung." Waijung with ARM Cortex-M4 based SPWM controller is new and unique for Induction motor speed control which gives feasible and significant solutions.

ARM Cortex-M4 processor is opted as it is a soft-core, and because of its unparalleled levels of compatibility, design reusability, and superior performance. It also provides an extensive range of IP cores with general architecture providing high performance, low power utility and offers many solutions for applications across the full performance spectrum of automotive control system with optimal cost.

The proposed scheme, which is based on a read-only memory (ROM) look-up table (LUT), is planned and as simulated in the processor to generate sinusoidal signals. The PWM signals generated by this system are called sinusoidal pulse width modulation (SPWM) signals. The generated pulses are having constant amplitude with different duty cycles for each period. The width of these pulses is suitably modulated to get inverter output. This method provides many advantages like enhanced stability and high-performance control over the sinusoidal signals generated. The utility of the system developed is appropriately shown by assessing the desirable performance in terms of total harmonic distortion (THD) over an extensive range of desired commands. Owing to its simplicity, it can be easily designed and realized in ARM Cortex-M4 processor. Due to less ripples and low THD values of this designed system, the consumption of electrical energy is less. Because of the smooth variation of speed control under different load condition, the system will be redeemed from voltage swell. So it avoids wastage of electric power .Hence the consumption of electrical energy of the entire system is highly economical.

This paper is structured as follows: In Section 1 is introduction. In Section 2, salient features of scalar control are discussed. Section 3, significance of ARM Cortex-M4 is described. In Section 4, the proposed design of the open-loop system is presented. In Section 5, the proposed design of closed-loop system is presented. Section 6, the technique used for modulation and pattern generation are discussed. In Section 7, software used and the way of implementation done in hardware are described. In Section 8, Experimental results are discussed. Lastly, conclusions are given in Section 9.

2. Salient Features of Scalar Control

The base speed of a motor depends on the supply frequency and the poles numbers. Because the latter is determined by design, the speed of the IM can be altered by changing the supply frequency. In an IM the torque production is directly proportional to the ratio of supply voltage and the frequency applied (V/f). By keeping the ratio of voltage and frequency constant, but changing the voltage and frequency, the torque produced can be kept constant during the

entire speed range. This is the fundamental characteristic of (V/f) control [1, 3, 27].

The speed-torque characteristics of the (V/f) control scheme show the following:

- The requirement of starting current is lesser.
- Throughout entire speed region the torque produced is maintained constant.
- Increasing and decreasing rate of speed of IM can be controlled by the supply frequency.

Stator Voltage (V) α [Stator Flux (Φ)] × [Angular Velocity (ω)]

$$V \alpha \Phi \times 2\pi f \quad (1)$$

$$\Phi \alpha V/f \quad (2)$$

This article shows 3.8 as (V/f) ratio used to produce constant torque with a wide a range of speed control.

3. ARM Cortex-M4

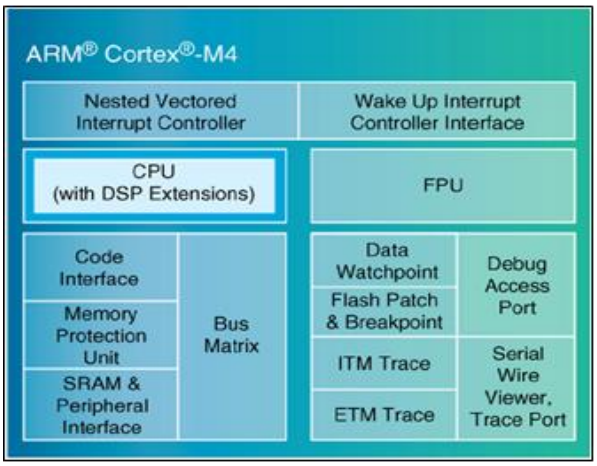

Fig. 1. Structural block diagram of ARM Cortex-M4 MCU.

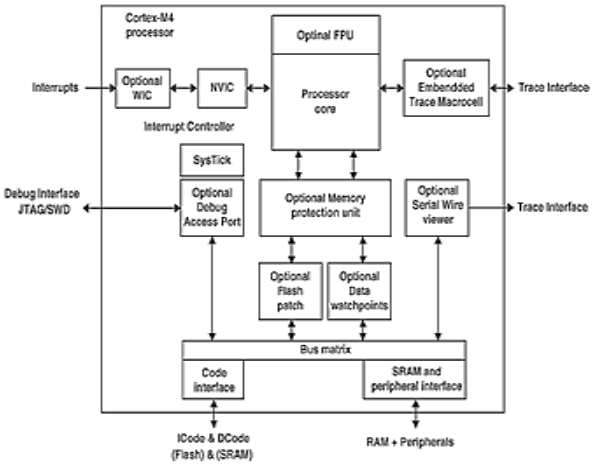

Fig. 2 . Functional block diagram of the ARM Cortex-M4 CPU.

The development of a programming code becomes easy because of ARM, which is also known as an advance reduced instructed set computing (RISC) microprocessor [28]. Indeed, an embedded system may be described as a system with some CPUs (central processing units) with some memory subsystems, I/O ports, and possibly several peripheral devices put together into a single semiconductor chip in order to design an intelligent control unit, known as a microcontroller unit (MCU). Recently, various types of embedded systems or MCUs are conceived and developed. Among the MCU family, ARM Cortex-M4 is one of the well-known MCUs.

The main advantages of this MCU are low power consumption, good controllability, and multi-functionality, better signal processing functionality, easy to use design and high efficiency. The ARM Cortex-M4 MCU, which belongs to ARM v7 family, is the latest product developed by ARM. However this processor is designed to satisfy the promising category of flexible solutions specifically targeting the motor control, power management, automotive, and industrial automation markets.

Therefore, to regulate the three-phase induction machine, an ARM Cortex-M4 processor was used in the programming application in this study. Figs 1 and 2 show the structural and functional block diagrams of the ARM Cortex-M4 MCU.

Specific feature/ functions of ARM Cortex-M4 MCU

- Although an ARM Cortex-M4 MCU does not have any memory, it offers different memory interfaces to the external flash memory and SRAMs.
- The maximum searchable memory space of an ARM Cortex-M4 MCU is up to 4 GB because of its 32-bit data length.
- It offers low power cost and efficient operation due to its AMBA (advanced microcontroller bus architecture) standard.
- Better interrupt response due to nested vectored interrupt controller.

4. Open-Loop System

The system consists of a command processing block, a V/f function block and PWM generator block embedded in ARM Cortex-M4. The ratio of voltage and frequency function calculates the magnitude of the voltage corresponding to that frequency. The SPWM is generated from the PWM generator block that is fed to trigger the inverter.

Fig. 3 shows the block diagram for open-loop control of IM using ARM Cortex-M4 processor.

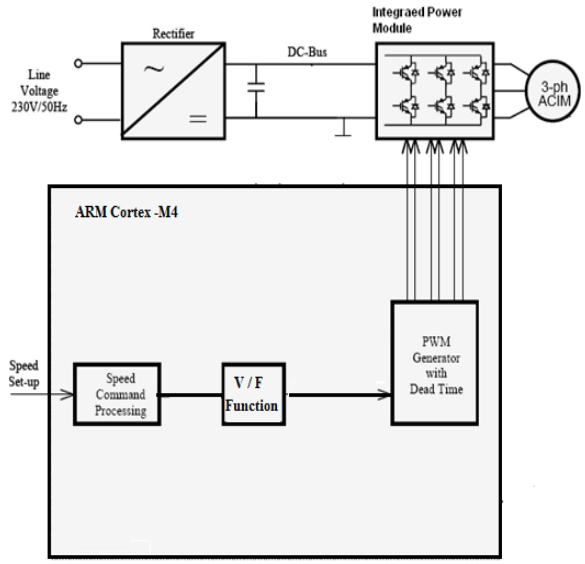

Fig. 3. Block diagram of the open-loop system.

5. Closed-Loop System

Fig. 4 shows the block diagram for closed loop control of IM using ARM Cortex-M4 processor. The system consists of feedback path and PI controller in addition to the open-loop system blocks embedded in ARM Cortex-M4 as a software module.

The "insulated gate bipolar transistor" (IGBT) is a switching device used in this system. To control the power delivered to the motor, the IGBT can switch ON and OFF several thousand times per second. The IGBT uses SPWM technique to produce a sine wave current at the desired frequency to the motor [29].

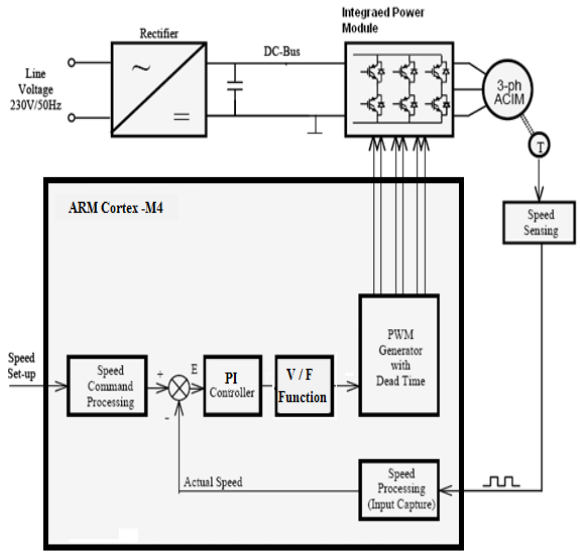

Fig. 4. Block diagram of the closed-loop system.

To process the error occurring between the actual and reference speeds, we can use a PI controller. The supply frequency is also varied by this process only. The amplitude of the supply voltage is varied by the voltage source inverter accordingly. Hence the V/f ratio remains constant. The experimental results have shown that the maximum torque remains constant throughout the entire speed range. Hence, the IM was completely used and successful speed control was achieved. Figs. 5 and 6 show the functional block diagrams of the open-loop and closed-loop systems.

6. Modulation Technique for SPWM

The most simple and useful method utilized for switching devices to generate a continuously varying analog signal is SPWM. This conversion technique has high electrical efficiency and is suitable to produce three perfect sinusoidal current wave-forms with 120-degree phase shift. If the two thyristor switches are turned on alternatively for equal timings, the duty cycle is 50% and the voltage across the load is zero. The average voltage is maximum across load when the duty cycle is 100%. This proves that the duty cycle is a key factor to produce the amplitude of average voltage [30, 31]. The shape of the load current is mainly based on the type of load. If the load is purely resistive, the shape of the load current wave-form would approximately be the same as that of the modulating square wave. However, if the load is inductive, the shape will be of the switching square wave, which is mainly based on the modulation of duty ratio. The load current shape is sinusoidal at the modulation frequency, lagging in phase only when the duty ratio varies sinusoidally in time.

The average voltage magnitude could be adjusted by altering modulation depth; e.g., an SPWM signal, which changes from 5% to 95%, yielding 90% modulation. This will yield an average voltage nine times higher than that given by a signal that changes only from 45% to 55%, giving only 10% modulation. Three such wave-forms are needed to drive a three phase IM motor that must be maintained at 120-degree phase shift, as shown in equations (3, 4, 5).

$$V_a(t) = V_m \sin(\omega t) \quad (3)$$

$$V_b(t) = V_m \sin(\omega t - 120) \quad (4)$$

$$V_c(t) = V_m \sin(\omega t + 120) \quad (5)$$

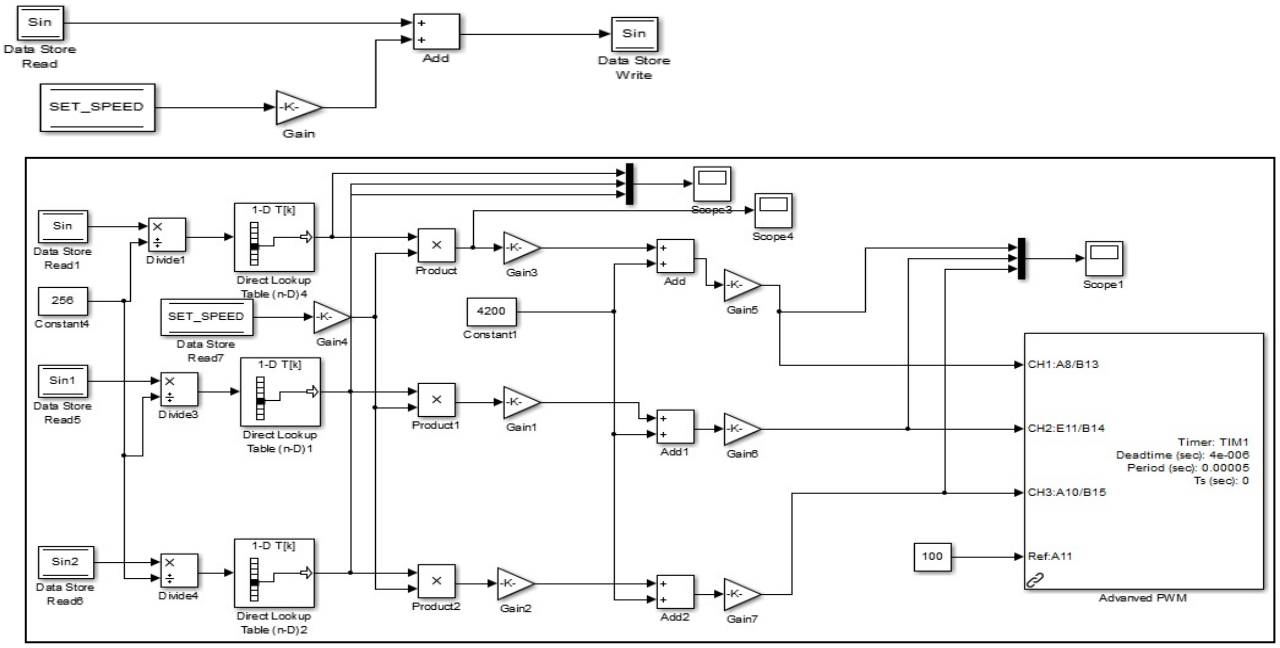

Fig. 5. Functional block diagram of the open-loop control system.

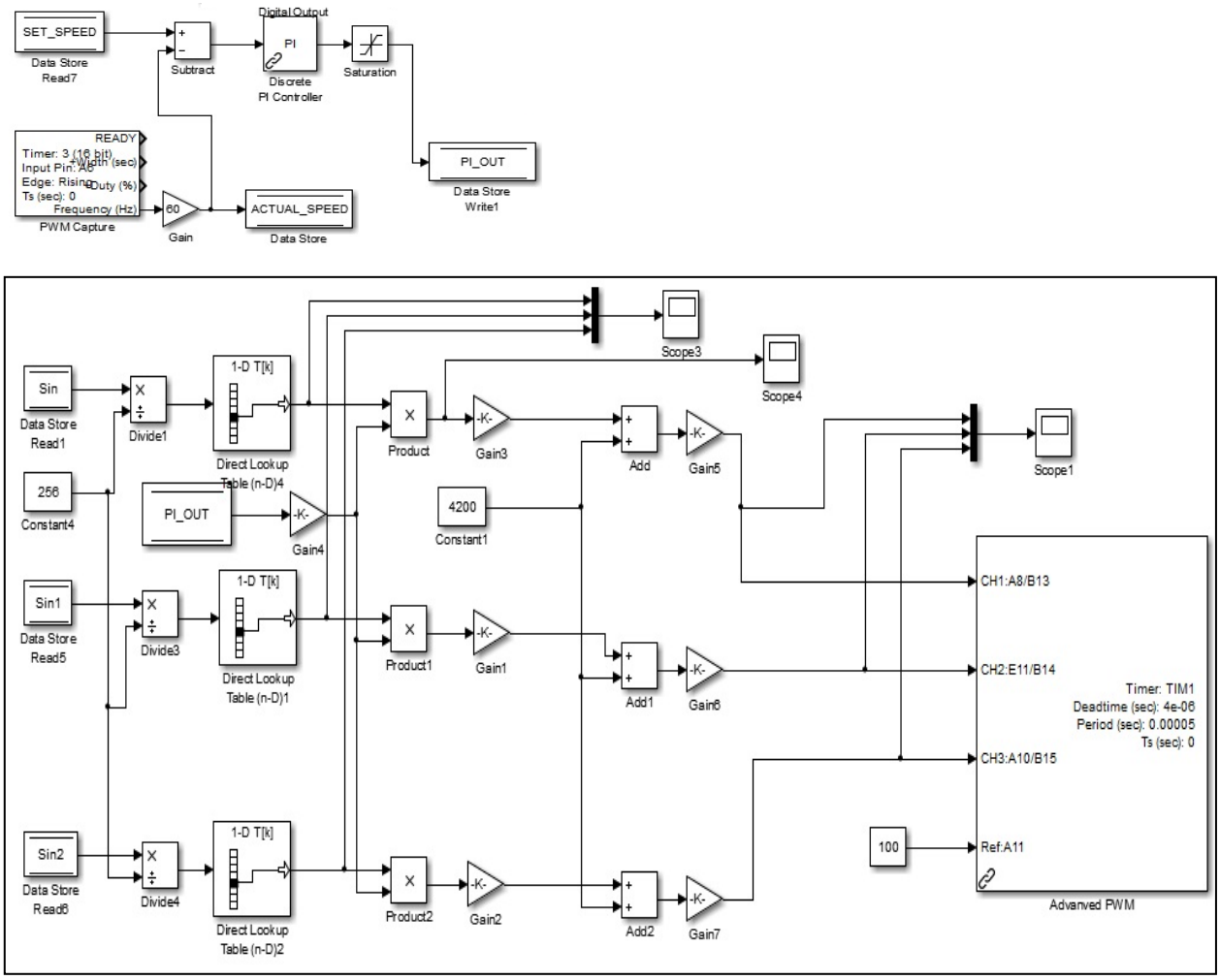

Fig. 6. Functional block diagram of the closed-loop control system.

The modulation depth must be changed according to the modulation frequency in order to maintain the magnetic flux in the motor at the desired level. Generally, the modulating frequency varies between 0 and 50Hz. The switching frequency chiefly depends on the switching devices used in the inverter. The sine wave-form can be stored in the LUT in terms of numerical values. The LUT can be read at three points to generate three sine waves that have 120- degree phase shift. The numeric values fetched from the LUT show the duty cycle an analogous to 100% modulation. To get the correct duty cycle for desired modulation depth, the fetched value from the LUT can be scaled down by equivalent manipulation technique.

The depth of modulation is obtained from the input frequency. The advanced PWM block-set computes the on-time for all the six power switches by implementing digital manipulation process to the internal LUT values. This process is cycled at regular intervals to generated SPWM pulses, which are shown in Fig. 6.The switching frequency of the IGBT is 10 kHz and the dead time is 4 µs.

7. Software and Hardware Implementation

The speed monitoring and speed control of IM is carried out by integrating hardware and software. VSCM4 is the STM32F407ZG controller-based embedded board that is used in this application. STM32F407ZG is a Cortex-M4F-based microcontroller. This board dedicates PWM, ADC, ETHERNET, LCD, UART, SPI_ADC, SPI_DAC, and DIGITAL input output sections. Figs 21 and 22 show the VSCM4 board and speed sensor. Following are the features of the STM32F407ZG microcontroller.

MATLAB 13.0 was used for complete development of the design. The graphical user interface (GUI) was also designed in MATLAB for real-time monitoring, which is shown in Fig 19.

7.1 Waijung software:

There may be two major concerns while implementing the real-time application using MATLAB/Simulink tool.

1. Interfacing hardware with MATLAB.
2. Time-sensitive applications.

To solve the concerns, Aimagin has made a customized block set named Waijung. This gives an opportunity to the user to interface the hardware with the MATLAB/Simulink. By using this Waijung block set, the user can realize a real system. It helps the whole process make fast and easy from design to implementation. So Waijung is a worth full addition to MATLAB/Simulink block-set.

First, the entire system is designed by Waijung block set in MATLAB 13.0. The code functionality is verified using simulation. The inputs and outputs of the design are mapped to the physical I/O pins of the ARM Cortex-M4 by explicit specification. At last the system design in MATLAB/Simulink is downloaded to the ARM Cortex-M4 board through JTAG (Joint Test Action Group). The set speed of the motor is given as input from the designed GUI through the Ethernet dynamically. The speed of the IM is sensed by the optical encoder and a sequence of pulses is generated. The sequential production of pulses is directly proportional to the speed of the IM. These pulses are given to the one of the counters of STM32F407ZG microcontroller which is in ARM Cortex-M4. Then the counted pulses are converted into digital value for converting back to frequency. The actual speed of the motor is displayed in rpm on the LCD. Then the PI control logic is applied by the microcontroller to calculate the error signal and generate the PWM signal to achieve the desired speed. Table 1 shows the specification of Microcontroller.

Table 1. Specification of Microcontroller

Microcontroller	STM32F407ZG
Operating Voltage	1.8 to 3.6V
Digital I/O Pins	140
Power consumption	108mA
Analog Outputs Pins	2 (DAC)
Flash Memory	1 MB
SRAM	192KB
Internal oscillator	16MHZ
Operating speed	168MHZ
ARM core	Cortex-M4F 32-bit

8. Experimental Results

Though the sinusoidal PWM approach decreases the harmonic current of the IM, the rms value is considerably reduced. It is noticed from the experimental results that when the inverter is supplied with a 220-Vrms line voltage, which provided 310 V dc in the capacitor filter bus, the rms voltage of the IM is decreased to about 190 V rms in 50 Hz. In this study, the V/f ratio was not adjusted again for low-speed operations. Therefore, IM operation was restricted to between 20% and 90% of its nominal speed.

The efficiency of the proposed system was determined by conducting the following experiments: (1) no load speed response related to reference; (2) speed response related to the reference step variations; (3) load response related to reference speed, THD; and,(4) response related to sudden applied load and release. Comparative analyses without controller and with controller (PI) were also carried out.

First, the driver circuit is connected to the programmed ARM Cortex-M4 kit. The PWM signals generated by the kit are tested with the help of a digital storage oscilloscope (DSO) for different amplitudes and frequencies. The desired dead band time of 4 µs is hard coded in the program itself. The generated PWM pulses from the ARM kit are shown in Fig. 7. Table 2 shows the specification of PI controller.

Table 2. Specification of PI Controller

Controller	K_p	K_i	Sampling time
PI	0.7	7	0.0001

The top and bottom IGBT's of the same leg are triggered by the generated PWM pulses. The applied two pulses are inverted with each other to avoid a shoot-through problem (i.e., both IGBTs of the same leg should not be turned ON at the same time). Fig. 8 shows the pulses for top two consecutive IGBT's (i.e., IGBT's 1 and 3). Similarly, Figs. 10 and 11 show the closed-loop system.

As in the case of the open-loop system, the actual speed response is closer to the set speed. The effective range of speed to be controlled is between 300 and 1400 rpm. If the reference speed is lower than 300 rpm, the amplitude of the modulating signal is less. This weaker amplitude signal is not capable enough to drive the IM. The reference speed is changed in the steps of 100 rpm to measure the voltage and corresponding frequency. The THD of Voltage and Current, ratio of voltage and frequency (V/f), torque, and actual speed for open- and closed-loop systems are given in Tables 3, 4 and 5. It is observed that the actual speed is exactly equal to the set speed in the closed-loop system and the torque is also constant throughout the entire speed range. This article shows 3.8 as (V/f) ratio used to produce constant torque. It could be inferred from the above experimental results that the smooth speed control of IM is achieved with an ARM Cortex-M4 processor. Figs. 13(a) and 14(a) show the hardware responses of the open-loop and closed-loop systems with no load without filter monitored in GUI. All others are hardware responses with filter.

8.1 Reference step response:

With this experiment, the IM was started with a defined speed of 1000 rpm. It was altered to 1200 and 1400 rpm with a uniform time interval. The open-loop and closed-loop responses associated with the reference step-up and down variation are given in Figs. 9 and 12. It is observed that the open loop has the speed error of 14 rpm whereas the closed loop has ±1rpm (tolerance).

8.2 No-load response:

Initially, when the motor is started with no load in open loop, the response reached the reference at 0.7s with ripples and also the speed is not settled at 1200 rpm (speed error 14rpm), which is shown in Fig. 13(a).

Figs. 13(b) and 14(b) are no-load speed responses with filter. Figs. 13(c) and 14(c) show the LCD display of open and closed loop speed.

Fig. 13(d) and (e) show the open-loop current response, Vrms, Irms, Hz measured in the DSO and a power-quality analyser. But, when the motor is started with no load in closed-loop (with PI), the response reached the reference at 0.5 s without peak over-shoot with ripples and also the speed is settled at 1200 rpm (speed error is ±1rpm), which is shown in Fig. 14(a). Fig. 14(d) and (e) show the closed-loop current response, Vrms, Irms, Hz measured in the DSO and the power quality analyser.

8.3 Dynamic response:

The experiments shown in Figs. 15(a) and 16(a) were conducted by starting the IM with a reference speed of 1200 rpm. A load of 1.2A was applied manually. It was observed that when the load torque is applied, the speed of the IM tends to reduce. As Fig. 15(a) is of an open-loop system, the speed is dropped to 1180 rpm (20rpm drop) and it is continuously running with the same speed. Throughout the experiment, the speed error is less than 14 rpm. Figs. 15(b) and (c) show the open-loop current response, Vrms, Irms, Hz measured in the DSO and the power-quality analyser. In the closed-loop system, the speed is dropped by 10 rpm at a moment, after applying the load of 1.2A at 2 s. The embedded PI system was able to correct the error by adjusting the voltage and frequency. The speed response is settled at 2.2s (Fig. 16(a)). During the test, the speed error observed by the PI controller was ±1 rpm, which shown in Fig. 14(c). Figs 16(b)and (c) show the closed-loop current response, Vrms, Irms, Hz measured in the DSO and the power-quality analyser. It is shown in Figs. 17 and 18 that the load of 1.2A is suddenly applied at 2 s and released at 6.5 s for both systems. It is clearly observed that the gain value of the PI controller was adjusted to give the best performance in the closed-loop system Fig. (18).

8.4 Comparative analyses with and without PI controllers:

To validate the proposed PI controller, the comparative analysis of the open and closed-loop systems was carried out. For the closed-loop system, the current THD came out to be 6% whereas for the open-loop system, it was equal to 6.3%. The detailed THD analysis is shown in Figs. 15(d) and (e), Figs. 16(d) and (e). The stator voltage wave form for open- and closed-loop is shown in Figs. 15(f) and 16(f).

PI controller discarded the overshoot and reduced the ripples compared to open-loop speed response. The settling time is lesser compare to that of the open-loop system. Therefore, the gain parameters of the controller were experimentally adjusted to produce a better performance in the experiments.

Table 3. THD of Voltage and Current

Load condition	Open loop		Closed loop	
1.2A	THD_V 7.0	THD_I 6.3	THD_V 6.4	THD_I 6.0

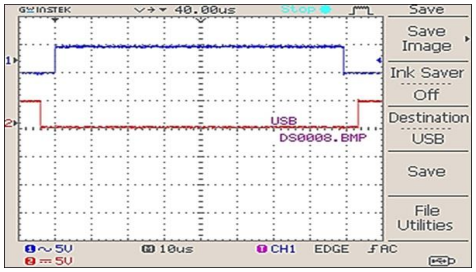

Fig. 7. Pulses fed to top and bottom IGBT's of one leg of the inverter open-loop system.
1div=5v; 1div=10µs

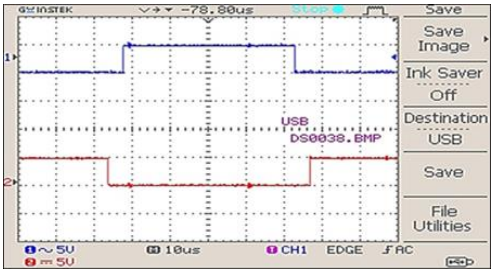

Fig. 10. Pulses fed to top and bottom IGBT's of one leg of the inverter closed-loop system.
1div=5v; 1div=10µs

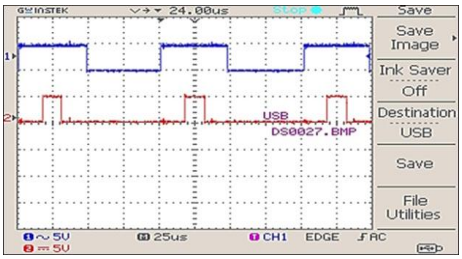

Fig. 8. Pulses for top two consecutive IGBT's (i.e., IGBT 1 and 3 open-loop systems).
1div=5v;1div=25µs

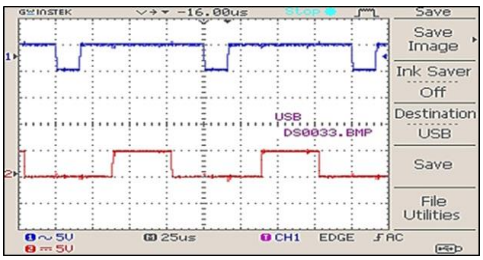

Fig. 11. Pulses for top two consecutive IGBT's (i.e., IGBT 1 and 3 closed-loop systems).
1div=5v;1div=25µs

Table 4. Experimental Results for 3.8 V/f ratio-: Open-Loop

V	F	V/F	Torque Nm	Set speed rpm	Actual speed rpm
166.12	42.676	3.89	1.56	1000	1013
175.8	45.701	3.85	1.57	1100	1113
183.5	47.455	3.87	1.57	1200	1215
188.2	48.823	3.85	1.55	1300	1312
192.9	49.667	3.88	1.58	1380	1394
194.7	50.56	3.87	1.59	1400	1412

Table 5. Experimental Results for 3.8 V/f ratio-: Closed-Loop

V	F	V/F	Torque Nm	Set speed rpm	Actual speed rpm
165.99	42.621	3.89	1.58	1000	999
174.00	45.150	3.85	1.58	1100	1100
181.30	46.693	3.88	1.57	1200	1200
187.70	48.635	3.86	1.56	1300	1300
191.40	49.454	3.87	1.56	1380	1379
193.38	50.094	3.86	1.58	1400	1400

Reference step response

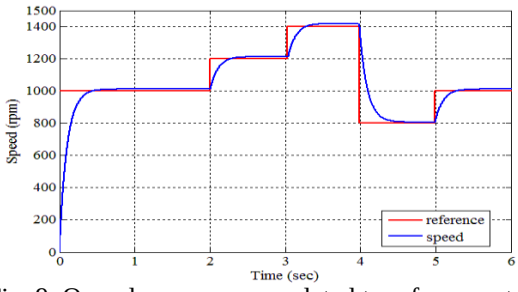

Fig. 9. Open-loop response related to reference step variation.

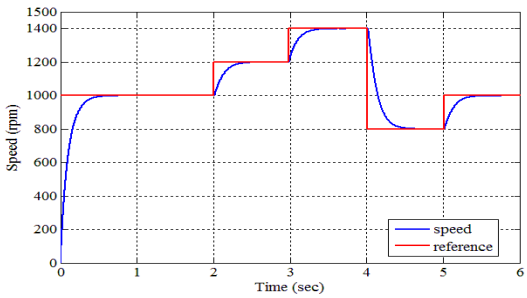

Fig. 12. Closed-loop response related to reference step variation.

No-load response

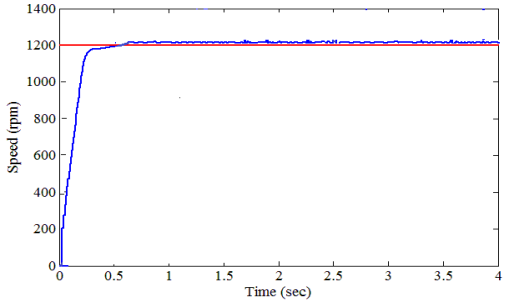

Fig. 13(a). Hardware speed response at no load without filter in the open-loop system.

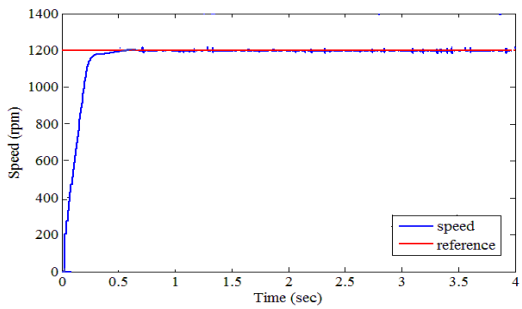

Fig. 14(a). Hardware speed response at no load without filter in the closed-loop.

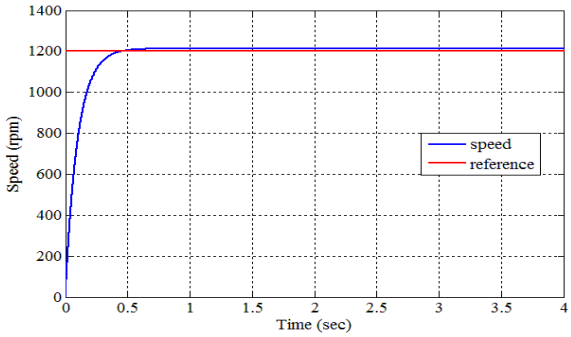

Fig. 13(b). Open-loop speed response at no load with filter.

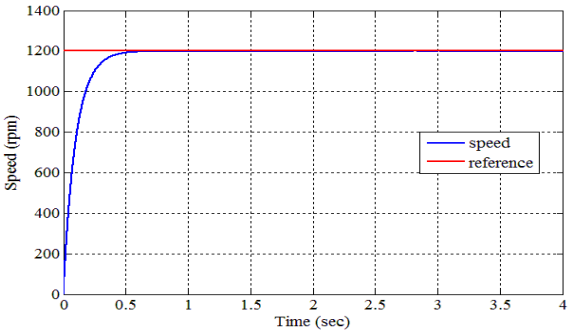

Fig. 14(b). Closed-loop speed response at no load with filter.

Fig. 13(c). Reference and actual speed display for open loop.

Fig. 14(c). Reference and actual speed display for closed-loop.

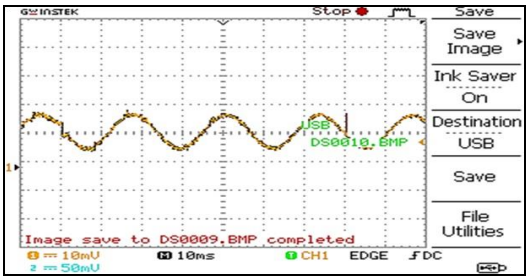

Fig. 13(d). Open-loop current response at no load (0.5A). CH1:10mv/div=1A, 10ms/div.

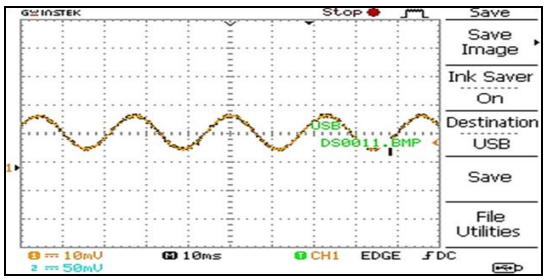

Fig. 14(d). Closed-loop current response at no load (0.5A). CH1:10mv/div=1A, 10ms/div.

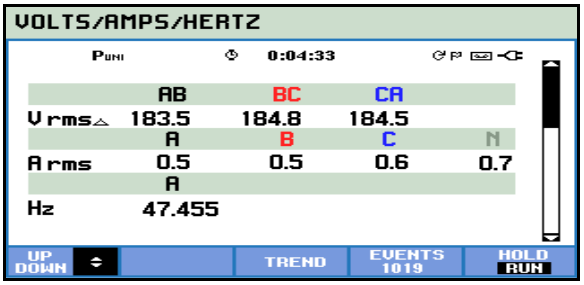

Fig. 13(e). Stator voltage, current and frequency for open-loop.

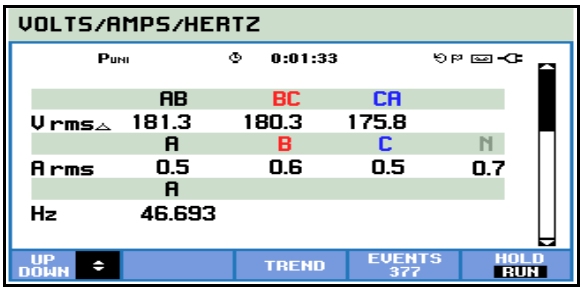

Fig. 14(e). Stator voltage, current and frequency for closed-loop.

Dynamic response

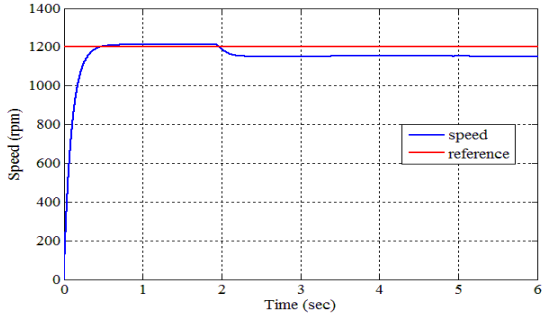

Fig. 15(a).Open-loop speed response of sudden applied load of 1.2A at 2s.

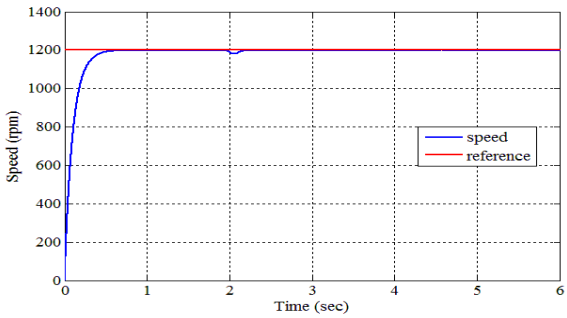

Fig. 16(a). Closed-loop speed response of sudden applied load of 1.2Aat 2 s.

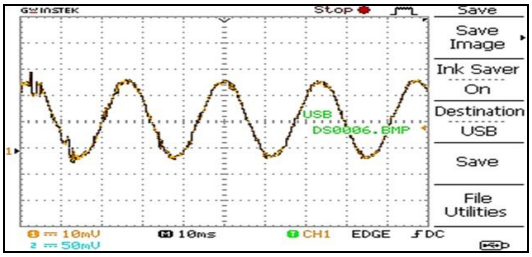

Fig.15 (b). Open-loop current response at 1.2A load. CH1:10mv/div, 10ms/div, 10mv/div=1A.

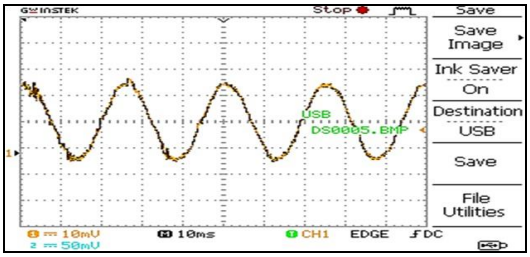

Fig. 16 (b). Closed-loop current response at 1.2A load. CH1:10mv/div, 10ms/div, 10mv=1A.

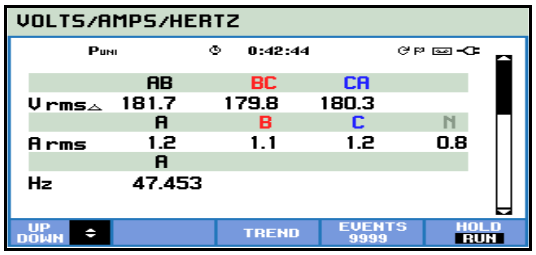

Fig. 15(c). Stator voltage, current and frequency for open-loop at the load of 1.2A.

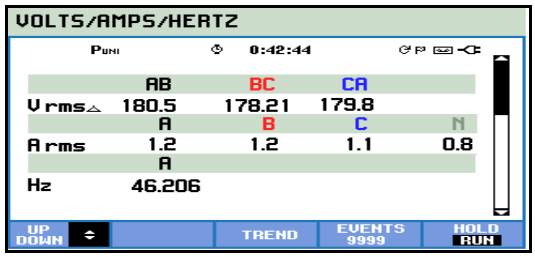

Fig. 16(c). Stator voltage, current and frequency for closed-loop at the load of 1.2A.

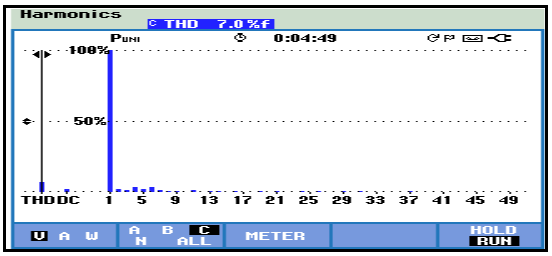

Fig. 15(d). Stator voltage THD at the load of 1.2A on open-loop.

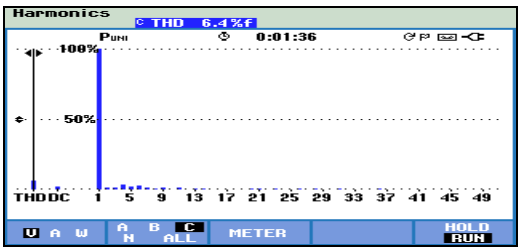

Fig. 16(d). Stator voltage THD at the load of 1.2A on closed-loop.

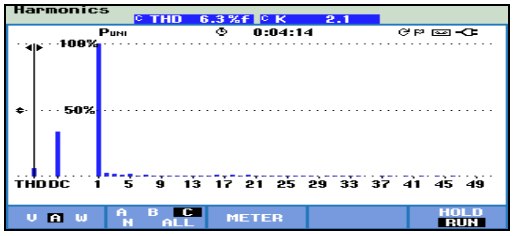

Fig. 15(e). Stator current THD at the load of 1.2 A on open-loop.

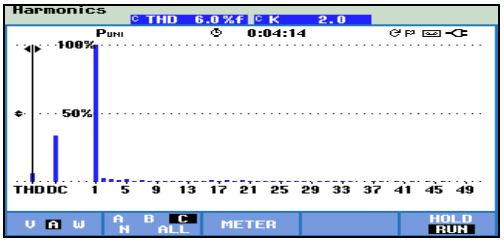

Fig. 16(e). Stator current THD at the load of 1.2A on closed-loop.

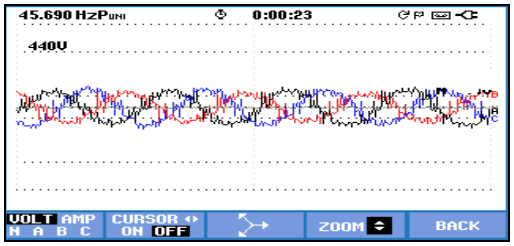

Fig. 15(f). Open-loop stator voltage.

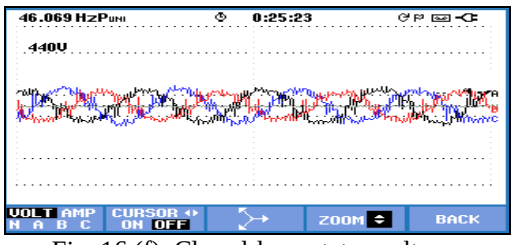

Fig. 16 (f). Closed-loop stator voltage.

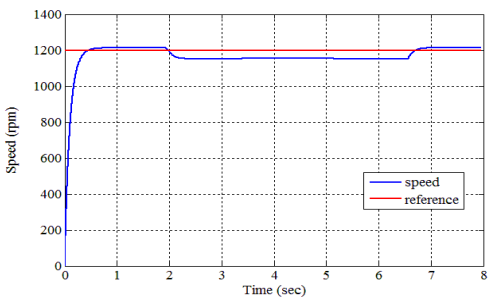

Fig. 17. Open-loop speed response of sudden applied load 1.2A at 2 s and released at 6.5 s.

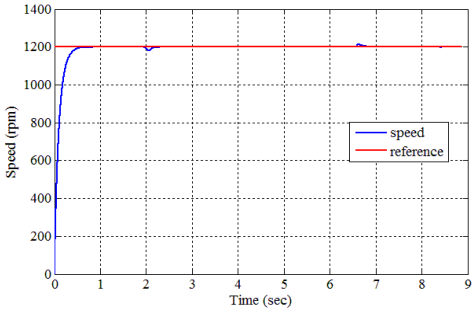

Fig. 18. Closed-loop speed response of sudden applied load 1.2Aat 2 s and released at 6.5 s.

Table 6. Specifications of the Hardware Setup used

Phase	3ph
Rated voltage	220 V (delta connected)
Rated current	2.4A
Power	1hp
Rated speed	1380

Table 7. Specifications of intelligent Power Module

IGBTs	6
Maximum Voltage	1200V
Maximum current	25A

Table 8. specification of sensor

Model	IP18305
Brown	+ive 5 to 30 V DC
Blue	-ive common
Black	output

9. Conclusion

An embedded, DSP-based IM speed control in open and closed-loop systems was implemented using STM32F407ZG a controller-based ARM Cortex-M4 processor. The unique features of Cortex-M4 processor support the system to reach its high controllability. Device selection and optimization allow the system to improve the performance. The open-loop response of an IM drive is not satisfactory for many industrial applications. It is satisfactory only if fluctuations can be tolerated or system components are designed and constructed to limit the parameter variations. When the load on the motor increases, the torque produced is also increased and the speed decreases.

The controllability of the motor in open-loop is limited with applied load condition that has been shown experimentally. To improve the controllability of the system, closed-loop control technique has been used. The PI controller is included in the feedback loop to adjust the duty cycle of the PWM signal output to achieve effective control over the motor. PI algorithm is embedded in the controller itself, which enables the on-board controller system yield a better steady state and transient response. This closed-loop control system has advantages such as improved accuracy, fast dynamic response, reduced THD, and reduced effects of load disturbances. In this work, SPWM method has been adopted, which gives excellent control of both torque and speed for low- and high-speed operations. We can able to control the speed of the motor at the rate of ±1rpm tolerance. By this way, the speed response attains the set speed within a second.

Experimental results showed that the new system makes the motor to run at constant speed (desired speed) irrespective of the load condition. Speed, code size and power consumption of the proposed controller were optimized to offer high level of controllability, flexibility and integration with minimum cost requirement. In this experiment, a flash-based controller was used. In the flash-based controller configuration, information is stored in on-chip flash cells. Once programmed, the configuration information is an inbuilt element of the controller structure and there is no need of external configuration data to be loaded at system power-up. This feature improves reliability and security levels of the system. Precise, fast, and effective speed reference tracking with minimum settling time and small steady-state error controls can be achieved by this closed-loop system on a chip (SoC) controller. This high-performance closed-loop system can be used in industrial applications such as process control, paper mills, steel mills, mining and smelting plants. This designed system leads economical consumption of electrical power because of the smartness involved in this system. Tables 6, 7, 8 show the specification of Induction motor, IPM and speed sensor.

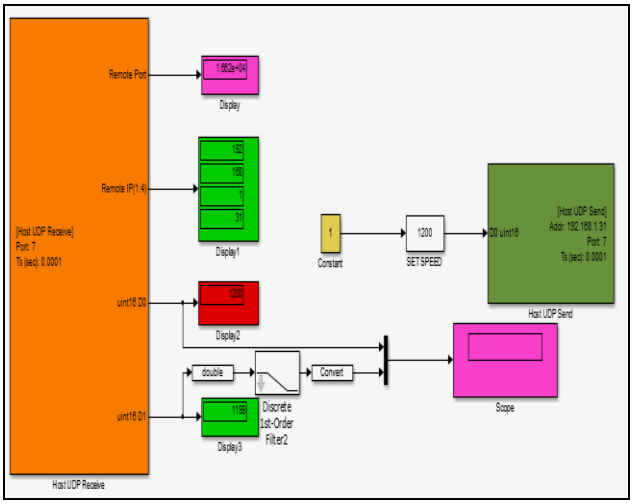

Fig. 19. Graphical user interface system.

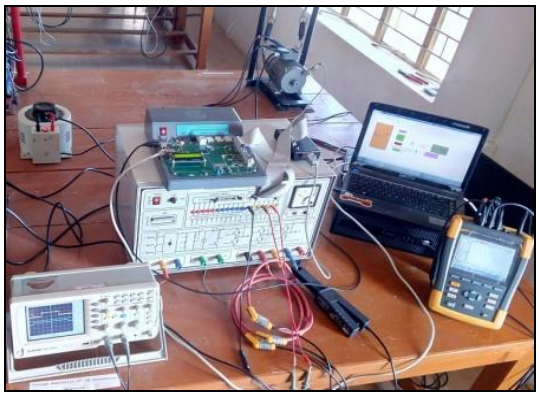

Fig. 20. Experimental setup.

Fig. 21. Cortex-M4 kit.

Fig. 22. Speed sensor.

References

1. R. Krishnan.: (*Electric Motor Drives—Modeling, Analysis, and Control*). Upper Saddle River, NJ:Prentice-Hall, 2001.
2. M. Trzynadlowski.: (*Control of Induction Motors*). New York: Academic, 2001.
3. B. Amin.: (*Induction Motors Analysis and Torque Control*). Springer, 2001, pp 12-64.
4. S. Maiti, C. Chakraborty, Y. Hori, and M. C. Ta.: (*Model reference adaptive controller-based rotor resistance and speed estimation techniques for vector controlled induction motor drive utilizing reactive power*), IEEE Trans. Ind. Electron. 2008, 55, (2), pp 594–601.
5. B. Singh, G. Bhuvaneswari, and B. Garg.: (*Harmonic mitigation in AC–DC converters for vector controlled induction motor drives*), IEEE Trans. Energy Convers, Sep. 2007, 22, (3), pp 637–646.
6. B. Karanayil, M. F. Rahman, and C. Grantham.: (*Online stator and rotor resistance estimation scheme using artificial neural networks for vector controlled speed sensorless induction motor drive*). IEEE Trans. Ind. Electron. Feb. 2007; 54, (1), pp167–176.
7. Tae-Chon, K. Yang-Won, H. Hyung-Soo, and W. Pedricz.: (*Design of neuro-fuzzy controller on DSP for real-time control of induction motors*), Proc. IFSA World Congr. 20th NAFIPS Int. Conf., 2001, 5, pp 3038–3043.
8. N. Islam, M. Haider, and M. B. Uddin.: (*Fuzzy logic enhanced speed control system of a VSI-fed three phase induction motor*), Proc. 2nd Int. Conf. Elect. Electron. Eng., 2005, pp 296–301.
9. B. Sharmila Y. Dharshan S.Vivek.: (*Fuzzy Logic Controller For Real Time Networked Control System*), Journal of Electrical Engineering, vol 17, 3rd edition, 2017.
10. D. G. Holmes, T. A. LipoThomas.: (*Pulse Width Modulation for Power Converters*), USA: IEEE Press, 2003.
11. F. Gonzalez-Espin, E. Figueres, G. Garcera, R. Gonzalez-Medina, and M. Pascual.: (*Measurement of the loop gain frequency response of digitally controlled power converters*). IEEE Trans. Ind. Electron. Aug. 2010, 57, (8), pp 2785–2796.
12. S. McKeown and R. Woods.: (*Low power field programmable gate array implementation of fast digital signal processing algorithms: Characterization and manipulation of data locality*), IET Comput. Digital Tech., Mar. 2011, 5, (2), pp136–144.
13. Eswaramoorthy, K. and Shunmughanaathan, V.K.: *(A Simple And Geometry Based Fast Space-Vector Pwm Technique For 15 Level Cascaded Multilevel Inverter With Reduction Of Switches),* Asian Journal of Research in Social Sciences and Humanities, 6(10), pp.2305-2320.
14. M. Suetake, I. N. da Silva and A. Goedtel.: (*Embedded DSP-based compact fuzzy system and its application for induction-motor V/f speed control*), IEEE Transact. Ind. Electron, Mar. 2011, 58, (3), pp 150-160.
15. Y.-Y Tzou.: (*A DSP-based robust control of an AC induction servo drive for motion control*), IEEE Transact. Control Systems Tech., Nov. 1996, 4, (6).
16. N. Saad, M. Arrofiq.: (*A PLC-based modified-fuzzy controller for PWM-driven induction motor drive with constant V/Hz ratio control*), Rob. Comput. Integ. Manuf., 2011, 28, (2), pp 95–112.
17. R. Arulmozhiyal and K. Baskaran.: (*Implementation of a fuzzy PI controller for speed control of induction motors using FPGA*), J. Power Elect., Jan. 2010, 10, (1).
18. B. Hariram, Dr. N. S. Marimuthu.: (*Evaluation of FPGA based speed control of induction motor*), Journal of Electrical Engineering, 2006.
19. Arzhang Yousefi-Talouki, Gianmario Pellegrino.*: (Sensorless Control of Matrix Converter-Fed Synchronous Reluctance Motors Based on Direct Flux Vector Control Method),* Journal of Electrical Engineering, vol 17, 2nd edition, 2017.
20. S. Datta and A. Chandra.: (Design and development of an 8 Bit microcontroller based space vector PWM inverter fed volt/Hz induction motor drive), 2nd Inter. Conf. Control, Instrum., Energy &Commun. (CIEC), 2016, pp 353-357.
21. K. Kedjar and B. Al-Haddad.: (*DSP-based implementation of an LQR with integral action for a three-phase three-wire shunt active power filter*), IEEE Trans. Ind. Electron., Aug. 2009, 56, (8), pp 2821–2828.
22. Y.-Y. Tzou, M.-F. Tsai, Y.-F. Lin and H.Wu.: (*Dual-DSP fully digital control of an induction motor*), Proc. IEEE ISIE Conf. Rec.Warsaw, Poland, Jun, 17–20, 1996, pp 673–678.
23. R. V. Aroca, L. M. G. Gonçalves.: (*Towards green data centers: A comparison of x86 and ARM architectures power efficiency*), J. Parallel Distrib. Comput., 2012, 72, pp 1770-1780.
24. M. I. Musyafani, F. Ardilla, M. M. Bachtiar.: (*Architecture design of low level control omni directional robot with RTOS-RTX ARM Cortex-M4*), Int. Electr. Symp.Denpasar, 2016, 91-196.
25. S. Incicco, F. Sala De Ferraris and Nicolas.: (*Real embedded navigation and control system for UAVs ARM Cortex-M4*), XVI Workshop Inf. Process. Control (RPIC), Cordoba.Argentina, 2015, pp 1-6.
26. N. Madhusudhana Reddy, K. NagabhushanRaju, C. Chandra Mouli and D. Chandrasekhar Reddy.: (*Design and implementation of ARM Cortex-based speed control of DC motor*), Int. J. Indus. Electr. and Control, 2012, 4, (2), 53-60.
27. M. S. Aspalli, R. Asha, P. V. Hunagund.: (*Three phase induction motor drive using IGBTs and constant V/F method*), Int. J. Adv. Res. Electri., Nov. 2012, 1, (5), 463-469.
28. J. Yiu.: (*The definitive guide to ARM Cortex-M0*). USA: Elsevier Science, 2011.
29. B. Biswas, S. Das, P. Purkait, M. S. Mandal and D. Mitra.: (*Current harmonics analysis of inverter-fed induction motor drive system under fault conditions*), Proc. Int. Multi conf. Eng. and Comp. Sci. vol. II, 2009 Mar 18- 20, Hong Kong, 2009.
30. W. Lin.: (*A new approach to the harmonic analysis of SPWM waves*), IEEE Proc., Int. Conf. Mechatronics Autom., 2006 June 25- 28, pp 390– 394.
31. Muthukumar Paramasivan, Melba Mary Paulraj, Sankaragomathi Balasubramanian.: (*Assorted carrier-variable frequency-random PWM scheme for voltage source inverter*), IET Power Electronics, vol. 10, No. 14, pp. 1993 – 2001, August 2017.